

Structural Characterization and Oxidation Reactivity of a Nickel(II) Acylperoxo Complex

Jun Nakazawa,* Shota Terada, Masaki Yamada, and Shiro Hikichi*

Department of Material and Life Chemistry, Kanagawa University, 3-27-1 Rokkakubashi, Kanagawa-ku, Yokohama 221-8686, Japan

S Supporting Information

ABSTRACT: The nickel(II)–acylperoxo complex $[\text{Ni}(\text{Tp}^{\text{CF}_3\text{Me}})(\kappa^2\text{-}m\text{CPBA})]$ ($\mathbf{1}^{\text{CF}_3\text{Me}}$) [$\text{Tp}^{\text{CF}_3\text{Me}}$ = hydrotris(3-trifluoromethyl-5-methylpyrazolyl)borate, $m\text{CPBA}$ = *m*-chloroperbenzoate] was isolated and fully characterized. The electrophilic oxygenation ability of $\mathbf{1}^{\text{CF}_3\text{Me}}$ toward sulfides and olefins was confirmed. The Michaelis–Menten-type behavior of thioanisole oxygenation indicates the existence of a pre-equilibrium of substrate association in the reaction. In addition, $\mathbf{1}^{\text{CF}_3\text{Me}}$ retains H-atom abstraction ability for hydrocarbons with activated methylene C–H bonds (e.g., fluorene). The oxidations of styrenes and these readily oxidizable hydrocarbons follow second-order kinetics, first-order each with respect to $\mathbf{1}^{\text{CF}_3\text{Me}}$ and substrate. The lack of clear acceleration in the decay of $\mathbf{1}^{\text{CF}_3\text{Me}}$ in the presence of substrates with high C–H bond dissociation energies (e.g., cyclohexane) suggests that another reaction pathway contributes through the O–O-cleaved intermediate.

Organic peroxycarboxylic acids, such as *m*-chloroperbenzoic acid (*HmCPBA*) and peracetic acid, are versatile oxidants and extensively utilized reagents for organic substrate oxygenation. *HmCPBA* has enough reactivity for O-atom transfer toward various organic compounds, including non-activated hydrocarbons, without the use of a catalyst. However, the combination of a transition-metal catalyst and *HmCPBA* leads to regio- and chemoselective oxygenation. In the catalytic process, it is considered that an initially formed metal–acylperoxo complex is a precursor to the actual active oxidants, namely, high-valent metal–oxo species formed via homolytic or heterolytic O–O bond cleavages.¹ In the case of heme iron complexes, the metal–acylperoxo species themselves also work as O-atom transfer reagents toward olefins.^{2,3} As a result, the chemical properties of *mCPBA* complexes of redox-active transition metals have attracted much attention. To date, fully characterized *mCPBA* complexes are still scarce. Especially, the substrate-oxidizing abilities of non-heme metal–*mCPBA* complexes remain to be clarified. The transfer of O atoms from Cu–*mCPBA* complexes to phosphine has been reported. However, these copper complexes are not very reactive.⁴

Recently, the selective hydroxylation of cyclohexane catalyzed by Ni(II) complexes with *HmCPBA* has been reported.⁵ While we were examining the reactivity of the active oxygen complexes of nickel with tridentate Tp^{R} ligands, where Tp^{R} denotes a substituted hydrotris(pyrazolyl)borate and R lists the non-hydrogen substituents (R = *iPr*, *iPr*₂Br, Me₂, and

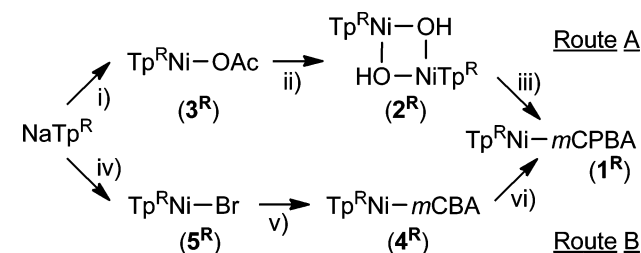
Me₂Br; see Chart 1), we detected thermally unstable Ni(II)–acylperoxo intermediates $[\text{Ni}^{\text{II}}(\text{Tp}^{\text{R}})(m\text{CPBA})]$ ($\mathbf{1}^{\text{R}}$).⁶ The

Chart 1. Abbreviations for the Tp^{R} Ligands

Tp^{R}	R ³	R ⁴	R ⁵
Tp^{iPr_2}	<i>iPr</i>	H	<i>iPr</i>
$\text{Tp}^{\text{iPr}_2\text{Br}}$	<i>iPr</i>	Br	<i>iPr</i>
Tp^{Me_2}	Me	H	Me
$\text{Tp}^{\text{Me}_2\text{Br}}$	Me	Br	Me
This work $\text{Tp}^{\text{CF}_3\text{Me}}$	CF ₃	H	Me

acylperoxo complexes $\mathbf{1}^{\text{R}}$ were formed by reaction of the dinuclear bis(μ -hydroxo)nickel(II) complexes $[(\text{Ni}^{\text{II}}\text{Tp}^{\text{R}})_2(\mu\text{-OH})_2]$ ($\mathbf{2}^{\text{R}}$) with stoichiometric amounts of *HmCPBA* (Scheme 1, route A). The thermal stability of $\mathbf{1}^{\text{R}}$ depends on

Scheme 1. Preparation of $\text{Tp}^{\text{R}}\text{Ni}^{\text{II}}$ Complexes^a



^a*mCBA* and *mCPBA* indicate *m*-chlorobenzoate and *m*-chloroperbenzoate, respectively. Reaction conditions: (i) Ni(OAc)₂; (ii) NaOH; (iii) *HmCPBA*; (iv) NiBr₂; (v) *KmCBA*; (vi) *HmCPBA*.

the electronic nature of the R⁴ group on the Tp ligand: the complex $\mathbf{1}^{\text{Me}_2\text{Br}}$ bearing the electron-withdrawing bromine group is more stable than the nonbrominated derivative $\mathbf{1}^{\text{Me}_2}$. Interestingly, the acylperoxo species $\mathbf{1}^{\text{R}}$ have the potential to abstract a hydrogen atom from the aliphatic C–H group, as evidenced by the kinetic isotope effect during the self-decomposition of $\mathbf{1}^{\text{R}}$ in CH₂Cl₂/CD₂Cl₂. We have not been able to isolate $\mathbf{1}^{\text{R}}$ to date. Not only does its structure remain to be characterized, but the nature of its oxidizing abilities toward various external substrates other than alkanes remains to be clarified. In this work, we characterized in detail the molecular

Received: February 25, 2013

Published: April 5, 2013

structure and external substrate oxidizing behavior of a Ni(II)–*m*CPBA complex.

Our strategy for the isolation of a Ni(II)–*m*CPBA complex involved controlling the properties of the Ni-supporting Tp^{R} ligand. As mentioned above, the incorporation of electron-withdrawing groups (EWGs) on the pyrazolyl rings of Tp^{R} enhances the stability of **1**. In addition, steric hindrance and chemical stability (i.e., resistance to oxidation) of the substituent groups on Tp^{R} are critical. Bulky alkyl groups (e.g., isopropyl groups) at the R^3 position of the pyrazolyl rings wrap the O–O moiety of the metal-bound acylperoxide, stabilizing **1** and hindering the reaction with external substrates. Moreover, C–H bonds of the R^3 substituents are oxidized by a proximal oxidant (i.e., metal-bound acylperoxide or further activated species generated via O–O breaking) through intramolecular reaction. Therefore, in this study hydrotris(3-trifluoromethyl-5-methylpyrazolyl)borate ($\text{Tp}^{\text{CF}_3\text{Me}}$) was employed as the Ni-supporting ligand because the proximal trifluoromethyl groups exhibit an electron-withdrawing nature, high oxidation resistance, and moderate steric hindrance. The versatility of $\text{Tp}^{\text{CF}_3\text{Me}}$ for the stabilization of metal–dioxygen species was revealed by the $\text{Cu}_2(\mu\text{-}\eta^2\text{-}\eta^2\text{-O}_2)$ complex reported by Gorun and co-workers.⁷

Our first attempt to synthesize an acylperoxo complex with $\text{Tp}^{\text{CF}_3\text{Me}}$ (**1** ^{CF_3Me}) in a manner similar to that used to form the reported **1** ^{R} (i.e., dehydrative condensation between the Ni(II)–hydroxo species and *Hm*CPBA; route A in Scheme 1)⁶ failed because of the insolubility of the putative Ni(II)–hydroxo complex **2** ^{CF_3Me} formed by the reaction of the Ni(II)–acetato complex $[\text{Ni}^{\text{II}}(\text{Tp}^{\text{CF}_3\text{Me}})(\text{OAc})]$ (**3** ^{CF_3Me}) with aqueous NaOH. Therefore, we selected an *m*-chlorobenzoate (*m*CBA) complex, $[\text{Ni}^{\text{II}}(\text{Tp}^{\text{CF}_3\text{Me}})(\text{mCBA})]$ (**4** ^{CF_3Me}), as a precursor to **1** ^{CF_3Me} because exchange of the *m*CBA ligand with *m*CPBA on the Ni(II) center might occur during the turnover process in catalytic alkane oxidation by Ni/*m*CPBA systems (route B in Scheme 1).⁵ **4** ^{CF_3Me} was prepared from bromido complex **5** ^{CF_3Me} by ligand exchange with *Km*CBA.⁸ As we expected, the reaction of **4** ^{CF_3Me} with a small excess (~2 equiv) of *Hm*CPBA in CH_2Cl_2 at $-40\text{ }^\circ\text{C}$ allowed a perfect conversion to **1** ^{CF_3Me} . Monitoring of the UV–vis spectral changes revealed an increase in absorbance at 375 nm, which was attributed to **1** ^{CF_3Me} , as the 408 nm band of **4** ^{CF_3Me} decreased with an isosbestic point at 395 nm. Surprisingly, this titration experiment was reproducible at room temperature, indicating the high thermal stability of the formed **1** ^{CF_3Me} [Figure S2 in the Supporting Information (SI)].

After the volatiles were removed from the reaction mixture of *Hm*CPBA (2.7 equiv) and **4** ^{CF_3Me} in CH_2Cl_2 , the dissociated *Hm*CBA and the remaining excess *Hm*CPBA were washed out with H_2O and EtOH. The agreement between the UV–vis spectra of the redissolved isolated solid and the final species in the above-mentioned titration in CH_2Cl_2 suggests that isolation was achieved (Figure S4). Recrystallization of the resulting green-blue solid from CH_2Cl_2 /*n*-hexane yielded a single crystal of **1** ^{CF_3Me} suitable for X-ray analysis (Figure 1 and Table S3 in the SI).^{8,9} The oxidation state of the Ni center is +2, and **1** ^{CF_3Me} is a neutral complex, as evidenced by the absence of any counterions in the crystal lattice. The Ni center in **1** ^{CF_3Me} is supported by a donor set containing three N atoms and two O atoms. The O–O bond length [1.443(3) Å] falls in the typical range for peroxide O–O lengths (Figure S4).^{3,4a,10} The coordination mode of *m*CPBA is κ^2 , as indicated by the bond lengths of the percarboxylate moiety [Ni1–O1, Ni–O3, and

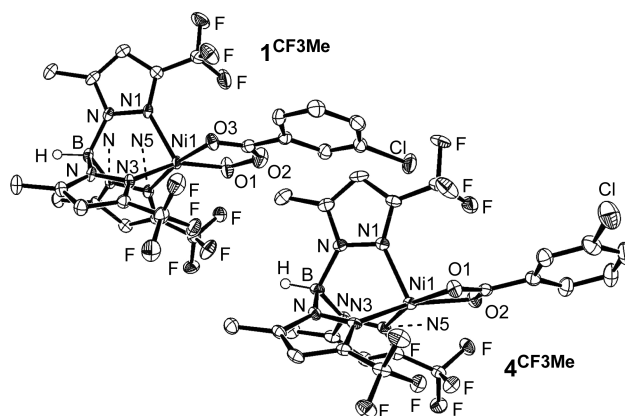
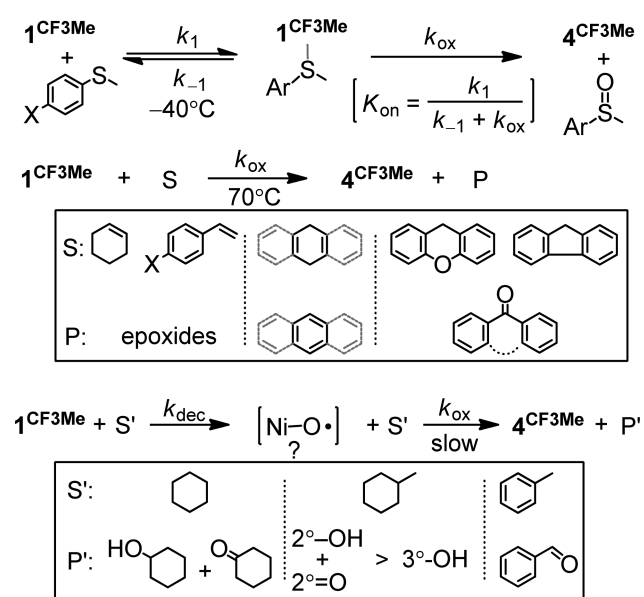


Figure 1. ORTEP diagrams of the complexes **1** ^{CF_3Me} and **4** ^{CF_3Me} with 50% thermal ellipsoids. H atoms on the carbon backbones have been omitted for clarity.

O3=C16 = 1.914(2), 2.040(2), and 1.223(3) Å, respectively]. The Ni–N(Tp) lengths in **1** ^{CF_3Me} [Ni1–N1, Ni1–N3, and Ni1–N5 = 2.037(2), 2.041(2), and 2.058(2) Å, respectively] are comparable to those in **4** ^{CF_3Me} , where the Ni center is supported by the tridentate $\text{Tp}^{\text{CF}_3\text{Me}}$ ligand and the κ^2 -binding *m*CBA ligand. The geometry of the nickel center of **1** ^{CF_3Me} is slightly distorted from square-pyramidal ($\tau = 0$) toward trigonal-bipyramidal ($\tau = 1$), as indicated by its τ value of 0.26. The Ni–*m*CPBA site is fully surrounded by CF_3 groups. These structural characteristics are consistent with the following observed spectroscopic properties:⁸ Paramagnetically shifted ¹H NMR signals of **1** ^{CF_3Me} assignable to the protons of the $\text{Tp}^{\text{CF}_3\text{Me}}$ and *m*CPBA ligands support the high-spin configuration ($S = 1$) of the distorted five-coordinate Ni(II) center (Figures S5 and S6). Coordination of the carbonyl moiety of the acylperoxo ligand leads to a red shift of the $\nu_{\text{C}=\text{O}}$ vibration to 1644 cm^{-1} in the IR spectrum, as found in the previously reported Tp^{R} derivatives (i.e., for **1** ^{Me_2} in CH_2Cl_2 solution at $-40\text{ }^\circ\text{C}$, $\nu_{\text{C}=\text{O}} = 1646\text{ cm}^{-1}$) (Figures S7–S9).^{4,6,11}

The oxidation reactivity of the isolated Ni(II)–acylperoxo complex **1** ^{CF_3Me} for external substrates in aprotic solvents ($\text{CF}_3\text{C}_6\text{H}_5$, toluene, benzene) was studied by kinetic analysis using UV–vis spectroscopy and product analysis using GC (Scheme 2).⁸ Without any substrate, the complex **1** ^{CF_3Me} was thermally robust even at $70\text{ }^\circ\text{C}$ in benzene (first-order rate constant = $1.63 \times 10^{-5}\text{ s}^{-1}$), while **1** ^{Me_2} decomposed below $-20\text{ }^\circ\text{C}$.¹² This thermal stability of **1** ^{CF_3Me} is a result of the steric protection around the Ni center and the electron-withdrawing nature of the CF_3 groups in the $\text{Tp}^{\text{CF}_3\text{Me}}$ ligand. However, **1** ^{CF_3Me} behaved as an O-atom transfer reagent toward nucleophiles such as phosphine and sulfide under mild conditions. A reaction solution containing 10 equiv of thioanisole stoichiometrically formed MeS(=O)Ph (96%) and $\text{MeS(=O)}_2\text{Ph}$ (1%), and the use of 10 equiv of PPh_3 gave O=PPh_3 (103%), as determined by GC analyses (yields based on **1** ^{CF_3Me} ; Table S4). In fact, the decay of **1** ^{CF_3Me} was accelerated even at $-40\text{ }^\circ\text{C}$ in the presence of excess thioanisole. The pseudo-first-order reaction rate constant (k_{obs}) for the decay of **1** ^{CF_3Me} became saturated as the concentration of thioanisole increased, implying that the reaction of **1** ^{CF_3Me} and thioanisole proceeds through a Michaelis–Menten-type mechanism (Scheme 2 and Figures S10–S12).¹³ A Lineweaver–Burk-type plot ($1/[\text{thioanisole}]$ vs $1/k_{\text{obs}}$) gave values of the association equilibrium constant K_{on}

Scheme 2. Oxidation of Various Substrates Using $\mathbf{1}^{\text{CF}_3\text{Me}}$ as the Stoichiometric Oxidant

for the formation of a substrate adduct of $\mathbf{1}^{\text{CF}_3\text{Me}}$ and the rate constant k_{ox} for the subsequent sulfoxide formation (Figure 2a).

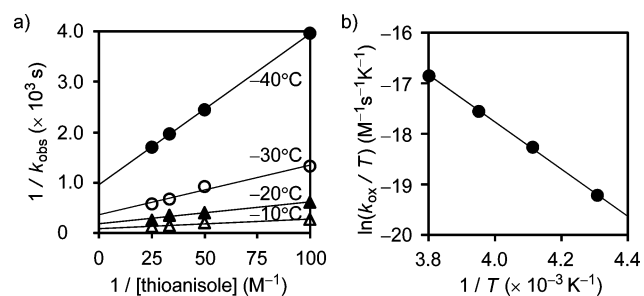


Figure 2. Plots of (a) $1/k_{\text{obs}}$ vs $1/[\text{thioanisole}]$ (Lineweaver–Burk plot) and (b) $\ln(k_{\text{obs}}/T)$ vs $1/T$ (Eyring plot) for the reaction of $\mathbf{1}^{\text{CF}_3\text{Me}}$ (1 mM) with thioanisole (5–40 mM) at -40 to -10 °C in toluene under Ar. The Eyring plot gave $\Delta H^\ddagger = 38.5 \text{ kJ mol}^{-1}$ and $\Delta S^\ddagger = -191 \text{ J K}^{-1} \text{ mol}^{-1}$.

The negative value of ΔS^\ddagger ($-191 \text{ J K}^{-1} \text{ mol}^{-1}$) derived from the Eyring plot suggested that the O-atom transfer from the Ni-bound acylperoxide to the S atom occurs directly (Figure 2b). The reactions of $\mathbf{1}^{\text{CF}_3\text{Me}}$ with other para-substituted thioanisoles ($\text{MeSC}_6\text{H}_4\text{-X}$; X = Br, Me, OMe) exhibited similar reaction profiles. Linear correlations between the substituent constants σ and the K_{on} and k_{ox} values, with negative values of the Hammett reaction constants ρ , indicated that the higher Lewis basicity of the substrate enhances the formation of the $\mathbf{1}^{\text{CF}_3\text{Me}}\cdot\text{MeSC}_6\text{H}_4\text{-X}$ adduct and that the Ni-bound acylperoxide shows an electrophilic nature (Figures S13 and S14).

The Ni(II)–acylperoxide complex $\mathbf{1}^{\text{CF}_3\text{Me}}$ also behaves as an electrophilic O-atom transfer reagent toward alkenes. Reactions of $\mathbf{1}^{\text{CF}_3\text{Me}}$ with 10 equiv of cyclohexene and styrene in $\text{CF}_3\text{C}_6\text{H}_5$ at 70 °C yielded the corresponding epoxides in 66 and 92% yield, respectively. The formation of small amounts of 2-cyclohexen-1-ol (4%)/2-cyclohexen-1-one (6%) and benzaldehyde (3%), respectively, might suggest the involvement of a small extent of H-atom abstraction (Table S4). The reactions of $\mathbf{1}^{\text{CF}_3\text{Me}}$ with a series of para-substituted styrenes ($\text{H}_2\text{C}=\text{CHC}_6\text{H}_4\text{-X}$; X = Br, H, Me, OMe) exhibited second-order

kinetics (Figures S15–S20). The negative value of ΔS^\ddagger ($-110 \text{ J K}^{-1} \text{ mol}^{-1}$) for the oxidation of styrene (X = H) indicates that the reaction proceeds through an associative transition state. The time course of changes in the UV–vis spectral pattern showed an isosbestic point, which may imply conversion from $\mathbf{1}^{\text{CF}_3\text{Me}}$ to $\mathbf{4}^{\text{CF}_3\text{Me}}$ without any intermediate. Also, the electrophilic nature of $\mathbf{1}^{\text{CF}_3\text{Me}}$ was evidenced by a negative ρ value (-1.35) derived from the Hammett plot of σ versus $\log k_{\text{ox}}$ (k_{ox} = second-order rate constant) at 90 °C.

Remarkably, $\mathbf{1}^{\text{CF}_3\text{Me}}$ can oxidize hydrocarbon substrates with activated methylene C–H bonds, such as 1,4-cyclohexadiene (CHD), 9,10-dihydroanthracene (DHA), xanthene, and fluorene, obeying second-order kinetics (Figures S21–S28). In the UV–vis spectrum of $\mathbf{1}^{\text{CF}_3\text{Me}}$ in the presence of a large excess of CHD, the $\mathbf{4}^{\text{CF}_3\text{Me}}$ band at 408 nm increased concomitantly with the consumption of $\mathbf{1}^{\text{CF}_3\text{Me}}$. No significant features were found at around 800 nm in our system; we attribute this result to the absence of putative high-valent Ni–O species arising from the cleavage of the acylperoxide O–O bond.¹⁴ The negative ΔS^\ddagger values for the reactions of the compounds with activated methylene C–H bonds indicated that $\mathbf{1}^{\text{CF}_3\text{Me}}$ works as the direct oxidant without an O–O-bond-cleaved intermediate (Figures S29–S32). The values of the second-order rate constants and C–H bond dissociation energies (BDEs) of these substrates are not correlated, which might be attributable to the steric effects of the CF_3 groups around the Ni center of $\mathbf{1}^{\text{CF}_3\text{Me}}$: less hindered CHD is more easily accessible to the acylperoxide ligand of $\mathbf{1}^{\text{CF}_3\text{Me}}$, leading to a faster reaction than with hindered DHA, although the latter has a lower BDE (Figure S33). It must be noted that no clear acceleration of the decay of $\mathbf{1}$ was observed in the presence of 1000 equiv of cyclohexane in benzene. The product analysis of the reaction of $\mathbf{1}^{\text{CF}_3\text{Me}}$ and methylcyclohexane indicated that the reaction proceeded in the somewhat sterically crowded coordination sphere of the Ni center (Table S4).⁶ Therefore, in the case of large-BDE substrates such as cyclohexane, another reaction pathway through the O–O-cleaved intermediates [i.e., high-valent Ni–O or Ni(II)–oxyl species] is dominant.

In conclusion, we have succeeded in fully characterizing the Ni(II)–acylperoxo complex. This thermally robust acylperoxide compound works as an O-atom transfer reagent toward nucleophilic sulfides and olefins and also is a genuine oxidant toward activated aliphatic C–H bonds.

■ ASSOCIATED CONTENT

Supporting Information

Experimental procedures, characterization data, and kinetic data. This material is available free of charge via the Internet at <http://pubs.acs.org>.

■ AUTHOR INFORMATION

Corresponding Author

jnaka@kanagawa-u.ac.jp; hikichi@kanagawa-u.ac.jp

Notes

The authors declare no competing financial interest.

■ ACKNOWLEDGMENTS

This work was supported in part by a Cooperative Research Program, “Network Joint Research Center for Materials and Devices” (2011169, 2012216, and 2012348), a Scientific

Frontier Research Project, and a Strategic Development of Research Infrastructure for Private Universities grant from the Ministry of Education, Culture, Sports, Science, and Technology of Japan. S.H. and J.N. also thank Kanagawa University for its financial support.

REFERENCES

- (1) Formation of reactive non-heme Fe=O species through O–O activation of putative Fe–*m*CPBA complexes: (a) De Oliveira, F. T.; Chanda, A.; Banerjee, D.; Shan, X.; Mondal, S.; Que, L., Jr.; Bominaar, E. L.; Munck, E.; Collins, T. J. *Science* **2007**, *315*, 835. (b) Lee, S. H.; Han, J. H.; Kwak, H.; Lee, S. J.; Lee, E. Y.; Kim, H. J.; Lee, J. H.; Bae, C.; Lee, S. N.; Kim, Y.; Kim, C. *Chem—Eur. J.* **2007**, *13*, 9393. (c) Ray, K.; Lee, S. M.; Que, L., Jr. *Inorg. Chim. Acta* **2008**, *361*, 1066. (d) van den Berg, T. A.; de Boer, J. W.; Browne, W. R.; Roelfes, G.; Feringa, B. L. *Chem. Commun.* **2004**, 2550. (e) Kodera, M.; Shimakoshi, H.; Kano, K. *Chem. Commun.* **1996**, 1737. (f) Kitajima, N.; Ito, M.; Fukui, H.; Moro-oka, Y. *J. Am. Chem. Soc.* **1993**, *115*, 9335.
- (2) Proposals for heme-Fe(III)–*m*CPBA species working as oxidants: (a) Suzuki, N.; Higuchi, T.; Nagano, T. *J. Am. Chem. Soc.* **2002**, *124*, 9622–9628. (b) Nam, W.; Lim, M. H.; Lee, H. J.; Kim, C. *J. Am. Chem. Soc.* **2000**, *122*, 6641–6647. (c) Lee, K. A.; Nam, W. *J. Am. Chem. Soc.* **1997**, *119*, 1916–1922.
- (3) The molecular structure and substrate oxidation abilities of the related peracetatoiron(III) complex have been reported: Zhang, X.; Furutachi, H.; Tojo, T.; Tsugawa, T.; Fujinami, S.; Sakurai, T.; Suzuki, M. *Chem. Lett.* **2011**, *40*, 515.
- (4) (a) Ghosh, P.; Tyeklar, Z.; Karlin, K. D.; Jacobson, R. R.; Zubieta, J. *J. Am. Chem. Soc.* **1987**, *109*, 6889. (b) Sanyal, I.; Ghosh, P.; Karlin, K. D. *Inorg. Chem.* **1995**, *34*, 3050. (c) Kitajima, N.; Fujisawa, K.; Moro-oka, Y. *Inorg. Chem.* **1990**, *29*, 357.
- (5) (a) Nagataki, T.; Ishii, K.; Tachi, Y.; Itoh, S. *Dalton Trans.* **2007**, 1120. (b) Nagataki, T.; Itoh, S. *Chem. Lett.* **2007**, *36*, 748. (c) Nagataki, T.; Tachi, Y.; Itoh, S. *Chem. Commun.* **2006**, 4016. (d) Balamurugan, M.; Mayilmurugan, R.; Suresh, E.; Palaniandavar, M. *Dalton Trans.* **2011**, *40*, 9413.
- (6) Hikichi, S.; Hanaue, K.; Fujimura, T.; Okuda, H.; Nakazawa, J.; Ohzu, Y.; Kobayashi, C.; Akita, M. *Dalton Trans.* **2013**, *42*, 3346.
- (7) Stabilization of Cu₂(μ-η²:η²-O₂) species by Tp^{CF₃Me} has been reported: (a) Hu, Z.; Williams, R. D.; Tran, D.; Spiro, T. G.; Gorun, S. M. *J. Am. Chem. Soc.* **2000**, *122*, 3556. (b) Hu, Z.; George, G. N.; Gorun, S. M. *Inorg. Chem.* **2001**, *40*, 4812.
- (8) See the Supporting Information.
- (9) Crystal Information Files for 5^{CF₃Me}, 4^{CF₃Me}, and 1^{CF₃Me} have been deposited with the Cambridge Crystallographic Data Centre (CCDC-924706–8).
- (10) O–O bond lengths in Fe–percarbonates and Ni–alkylperoxides: (a) Hashimoto, K.; Nagatomo, S.; Fujinami, S.; Furutachi, H.; Ogo, S.; Suzuki, M.; Uehara, A.; Maeda, Y.; Watanabe, Y.; Kitagawa, T. *Angew. Chem., Int. Ed.* **2002**, *41*, 1202. (b) Hikichi, S.; Okuda, H.; Ohzu, Y.; Akita, M. *Angew. Chem., Int. Ed.* **2009**, *48*, 188. (c) Hikichi, S.; Kobayashi, C.; Yoshizawa, M.; Akita, M. *Chem.—Asian J.* **2010**, *5*, 2086.
- (11) IR assignment of porphyrin-Fe–*m*CPBA: Groves, J. T.; Watanabe, Y. *Inorg. Chem.* **1987**, *26*, 785.
- (12) The thermal stability of 1^{CF₃Me} is comparable to that of HmCPBA.
- (13) Ligand exchange with the terminal O atom of *m*CPBA during the initial association process can be excluded because no immediate decrease in the peroxide-to-Ni ligand-to-metal charge-transfer band of 1^{CF₃Me} at 375 nm was observed in the UV–vis spectrum after the addition of thioanisole.
- (14) Pfaff, F. F.; Heims, F.; Kundu, S.; Mebs, S.; Ray, K. *Chem. Commun.* **2012**, *48*, 3730.